RESEARCH

Morphological study of remineralization of the eroded enamel lesions by tyrosine-rich amelogenin peptide

Mingzhu Wen[1], Qinghua Bai[1], Yiwei Li[1], Yaru Li[1], Dandan Ma[1] and Jinpu Chu[1*]

Abstract

Background Tyrosine-rich amelogenin peptide (TRAP) is the main amelogenin digestion product in the developmental enamel matrix. It has been shown to promote remineralization of demineralized enamel in our previous study. However, direct evidence of the effect of TRAP on the morphology and nanostructure of crystal growth on an enamel surface has not been reported. This study aimed to examine the effect of TRAP on the morphology of calcium phosphate crystals grown on early enamel erosion using a pH-cycling model.

Methods Eroded lesions were produced in human premolars by 30-second immersion in 37% phosphoric acid. Forty-five samples of eroded human premolar enamel blocks were selected and randomly divided into 3 groups: deionized water (DDW, negative control); 100 µg/mL TRAP, and 2 ppm sodium fluoride (NaF, positive control group). For 14 days, the specimens were exposed to a pH-cycling model. Using scanning electron microscopy (SEM) and atomic force microscopy (AFM) methods, the surface morphology, calcium-phosphorus ratio, and enamel surface roughness were examined. X-ray diffraction (XRD) and Fourier transform infrared spectroscopy (FT-IR) were used to assess crystal characteristics.

Results After pH-cycling, compared to the two control groups, the surface of the eroded enamel of the peptide TRAP group shows a large number of new, densely arranged rod-like crystals, parallel to each other, regularly arranged, forming an ordered structure, with crystal morphology similar to that of natural enamel. The crystals are mostly hydroxyapatite (HA).

Conclusion This study demonstrates that the peptide TRAP modulates the formation of hydroxyapatite in eroded enamel and that the newly formed crystals resemble natural enamel crystals and promote the remineralization of enamel, providing a promising biomaterial for remineralization treatment of enamel lesions.

Keywords Early enamel erosion, Morphological, Tyrosine-rich amelogenin peptide, Remineralization, Amelogenin

*Correspondence:
Jinpu Chu
cjp605@163.com
[1]The First Affiliated Hospital of Zhengzhou University, Zhengzhou, China

Introduction

The hardest tissue in the body, tooth enamel is a highly mineralized tissue that makes up the tooth's outermost layer. The basic component of it is the enamel rod. The enamel rods consist of nano-fibrous hydroxyapatite (HA) crystals. When exposed to acidic conditions (pH<5.5), hydroxyapatite crystals dissolve, enamel rods and internal rods are destroyed, and enamel is demineralized, leading to tooth erosion [1]. Dental erosion is the loss of dental hard tissue brought on by chemical processes without the presence of microbes. The etiology of this disease is usually acidic substances such as food, drink, and gastro-oesophageal reflux [2]. Dental erosion is a serious and common issue due to the rising popularity of acidic diets (especially drinks). Demineralized enamel cannot be fully repaired due to its non-regenerative nature. It must rely on a physicochemical procedure (remineralization) that uses inorganic components from solutions [3].

Now, methods including bioglass [4], chitosan [5], and fluoride [6] are now being used in the treatment of enamel erosion. Fluoride, in particular, is widely used in the treatment of enamel erosion. However, the newly precipitated apatite crystals on the surface of the enamel differ significantly in morphology and arrangement from the structure of natural enamel. Furthermore, dental and bone fluorosis caused by excessive fluoride intake cannot be ignored [7].

Enamel remineralization may now be safely encouraged by new biomaterials. Over the past 40 years, research has confirmed the function of amelogenin proteins in the mineralization of enamel. The interaction of matrix materials with amelogenin and fragments to mediate the synthesis of HA is continually being investigated [8].

The main enamel matrix protein, amelogenin, is necessary for optimal enamel development and is thought to be crucial for controlling the nucleation, growth, and morphology of enamel mineral phases. Amelogenin consists of a hydrophilic C-terminal domain, a hydrophobic central domain, and a tyrosine-rich N-terminal domain [9]. Studies have confirmed that the N- and C- termini domains are highly conserved and are crucial for the development of healthy enamel [10].

Full-length amelogenin was found to be less abundant during enamel development, mostly as an enzymatically cleaved polypeptide fragment [11]. Our previous study revealed that a recombinant amelogenin peptide (consisting of the C- and N- termini) induces remineralization of demineralized enamel. The peptide may serve as a calcium ion carrier and regulator for the formation of directly ordered crystals. This calcium carrier was associated with the S-16 monophosphate group (at the N- termini) in this peptide [12].

Tyrosine-rich amelogenin peptide (TRAP) is the main amelogenin digestion product in the developmental enamel matrix that is the N-termini domain of amelogenin. TRAP contains all the self-colonizing 'A-domains', the only phosphate group, and an exogenous lectin binding motif 'PYTSYGYEPMGGW ' of amelogenin [13].

Studies have shown that TRAP, like this peptide (consisting of the C- and N- termini), can encourage the remineralization of demineralized enamel [14]. However, direct evidence of the effect of TRAP on the morphology and nanostructure of crystal growth at a nanoscale level on an enamel surface has not been reported.

According to previous studies, changes in surface morphology are evident during enamel demineralization and remineralization [15]. Scanning electron microscopy (SEM) and atomic force microscopy (AFM) methods were used in this study to examine enamel surface morphology, calcium-phosphorus ratio and surface roughness. X-ray diffraction (XRD) and Fourier transform infrared spectroscopy (FT-IR) were used to assess crystal characteristics. Therefore, in this study, the effect of TRAP on the morphology and structure of crystal growth on eroded enamel surfaces was investigated, thus providing further evidence of the important role of TRAP in enamel remineralization.

Materials and methods

Peptide synthesis and characterization

TRAP was synthesized by standard solid-phase peptide synthesis from Synpeptide Co., Ltd., (Nanjing, China) that consists of residues (MPLPPHPGHPGYINFSPYEVLTPLKWYQNMIRHPYTSYGYEPMGGW). High-performance liquid chromatography (RP-HPLC) was used to purify it, and mass spectrometry was used to characterize it. The lyophilized peptides are dissolved in 4 mg/ml microporous purified water and stored at 4℃. Centrifuge the peptide stock solution before use (10,900 x g, 4 °C, 20 min).

Sample preparation

Extracted human teeth were collected according to the guidelines approved by the Ethics Committee of the First Affiliated Hospital of Zhengzhou University (2021-KY-1050-002). Premolars extracted for orthodontic reasons were obtained from the Department of Dentistry of the First Affiliated Hospital of Zheng University in the age group of 18–30 years. After extraction, soft tissue debris was removed, examined for fissures, dysplasia, and white spot lesions, and teeth were sterilized by cleaning with 5% NaClO for 1 h. A vertical incision was made along the buccal crown of the sample to obtain an enamel block 3×3×2 mm in size. The surface was smoothed with water-cooled silicon carbide paper of 400, 600, 800, 1000, 1200, 1500, 2000, 2500, 3000, and 4000 grit (Buehler Ltd.). The buccal surface was ultrasonically cleaned for 10 min to remove impurities. Randomly selected 15

Wen *et al. BMC Oral Health*   (2024) 24:1054

Page 3 of 11

samples and obtained baseline surface roughness, EDXS data, and raw image data of enamel blocks using SEM, AFM, FT-IR, and XRD prior to the formation of acid eroding. After that, all enamel samples were kept at 4 ℃ in a deionized water solution.

Eroded enamel preparation

Apply a gel of 37% phosphoric acid to the buccal surface of enamel blocks for 30 s and wash the surface of enamel blocks thoroughly with deionized water (DDW) [6]. After naturally drying, a double layer of acid-resistant nail polish was applied to the rest of the region, except the buccal surface. In the same way as before acid eroding, randomly selected 15 samples and obtained the enamel's surface roughness, EDXS data, and image data of enamel blocks using SEM, AFM, FT-IR, and XRD after the formation of acid eroding.

pH-cycling regime

Standard pH-cycling was performed according to a previously reported protocol [16]. Randomly selected 45 samples and divide the enamel blocks into 3 groups of 15 samples each. The groups were divided as follows: Group 1: DDW group (negative control group); Group 2: 100 µg/mL tyrosine-rich amelogenin peptide (TRAP); Group 3: 2 ppm NaF (positive control group). Three research groups had their enamel samples submerged in the treatment solution four times a day for 10 min each at 8:00, 9:00, 15:00, and 16:00. The acid challenge was carried out by immersion for two hours between 11:00 and 13:00 in a demineralization solution containing 2.2 mmol/L $Ca(NO_3)_2$, 5 mmol/L NaN_3, 50 mmol/L acetic acid, and 2.2 mmol/L KH_2PO_4 (pH=4.5). Samples were submerged in the remineralization solution for the remaining period, which included the following ingredients: 5 mmol/L NaN_3, 20 mmol/L HEPES, 130 mmol/L KCl, 0.9 mmol/L KH_2PO_4, and 1.5 mmol/L $CaCl_2$ (pH=7.0) [17]. In a tank that was sealed and continuously stirred with a low-speed magnetic stirring at 100 rpm while keeping the temperature at 37 ℃, the cycle was repeated for 14 days. The samples were carefully rinsed with deionized water following each procedure. Prepare and replace fresh solutions daily. After pH-cycling for 14 days, washed well with deionized water and allowed to air dry naturally.

Scanning electron microscopy (SEM) and energy-dispersive X-ray spectroscopy (EDXS)

After pH-cycling remineralisation, five samples were randomly selected from each group to examine the surface crystal using a Scanning electron microscopy (SEM, Gemini 300 M, Zeiss, Germany). Using an Oxford Quorum SC7620 sputter coater at 10 mA, the samples were collected, adhered directly on the conductive adhesive, and coated with gold for 45 s. The surface morphology of

the enamel mass was then photographed using the SEM at 3 kV of accelerating voltage. Energy spectrum mapping tests were carried out with a 15 kV EDXS detector (Smartedx detector, Germany) to The Ca and P ratios (At. %) in the samples after treatment with remineralizes were assessed. Data were calculated as mean and standard deviation and expressed as mean±standard deviation. On the basis of these EDXS data, potential mineral phases were predicted. On the basis of these EDXS data, potential mineral phases were predicted.

Atomic force microscopy (AFM)

After pH-cycling remineralisation, five samples were randomly selected from each group to observe the surface morphology of the enamel using an atomic force microscope (Bruker Dimension Icon AFM, Germany) and to determine the surface roughness. The samples were fixed on slides and five loci were randomly selected for each sample and photographed in intermittent contact mode using an AFM instrument with a scanning area of 30 µm x 30 µm. NanoScope Analysis software was used to analyze the images and the origin software to plot them.

Fourier transform infrared spectroscopy (FT-IR)

After pH-cycling remineralisation, two samples were randomly selected from each group, and the surface crystals were analysed for composition using a Fourier transform infrared spectrometer (FT-IR, Nicolet iS10, USA). In a dry environment, the ATR accessory was placed in the optical path of the IR spectrometer, the air background was scanned, and the sample surface was pressed against the crystal surface of the ATR accessory, and then the infrared spectra of the sample were tested and captured in the wave number range of $2000-500\ cm^{-1}$, with a resolution of $4\ cm^{-1}$, and the number of scans was 32.

X-ray diffraction (XRD)

After pH-cycling remineralisation, three samples were randomly selected from each group, and the mineral phase of the new crystals were analysed for composition using a X-ray diffraction analysis(Rigaku Ultima IV, Japan). By using CuKa (λ=1.5418 Å) radiation at 40 mA and 40 kV, the samples were examined using XRD. Data were gathered over a 2Ɵ angle range of 20–70°at a scan rate of 350 s/step and in 0.02° steps. The chemical phases were indexed using the International Centre for Diffraction Data (ICDD, PDF-2 release 2004 version). Diffractograms were analyzed using MDI Jade v6.0 and plotted using origin software.

Statistical analysis

All data were statistically analyzed using SPSS 21.0 (IBM, Chicago, IL, USA) and plotted using origin software. The enamel surface roughness data before and after

Wen *et al. BMC Oral Health*   (2024) 24:1054

Page 4 of 11

acid eroding and after remineralization were compared by t-test. After remineralization, statistical significance between groups was assessed using analysis of variance and Bonferroni correction. $P < 0.05$ was used as the significance criterion.

Results

SEM morphology

Figure 1 showed the surface morphology of the enamel samples. The surface was analyzed for elemental composition using EDXS. Newly deposited crystals were observed in all groups, but their morphology, growth direction, and distribution on the enamel surface differed after pH-cycling for 14 days. The intact enamel surface was flat and a few scratches were visible. EDXS investigation of the surface's elemental composition showed a Ca/P ratio of 1.66 ± 0.06 (Fig. 1A, B). The eroded enamel surface had an overall fish-scale appearance, with a preferential loss around the enamel prisms, protrusion of demineralized prismatic nuclei towards the original enamel surface, and discontinuity and fragmentation of crystals at the surface. The enamel surface was analyzed for elemental composition and content using EDXS and a Ca/P ratio of 1.61 ± 0.08 was obtained (Fig. 1C, D). In all three groups, the enamel surface had a coating of precipitated crystals after pH-cycling remineralization. In contrast to the other groups, the surface of the enamel in the DDW group was characterized by large holes and pits, which were broadly visible as enamel prisms, with no obvious restoration of the interstitial enamel rods. Loose and disordered accumulations of fragmentary short rod-shaped crystal particles were visible on magnification (Fig. 1E). The Ca/P ratio was determined by elemental analysis to be 1.61 ± 0.12, probably a mixed mineral composition of calcium-phosphate transition phases and HA (Fig. 1F) [15]. The remineralized enamel surface of the TRAP group was relatively flat, the precipitates were connected in sheets and covered some of the pores and pit areas. The damaged enamel interstices were well repaired, and a few pits were visible. On magnification, many new, densely arranged rod-like crystals were visible on the surface, parallel to each other, regularly arranged and forming an ordered structure, closely mosaic with the enamel crystals at the base. It was difficult to distinguish between the natural enamel and the new crystals in terms of morphological and structural features, suggesting that the new crystal morphology is similar to that of the natural enamel crystals (Fig. 1G). The Ca/P was 1.65 ± 0.23, close to the ideal HA ion ratio of 1.67 (Fig. 1H) [15]. Fluoride addition increased the extent of enamel surface repair. The surface of the enamel was flat and the pits were largely invisible (Fig. 1I). Magnification of the rougher areas reveals a looser arrangement of relatively regular columnar crystals. Magnification of the flat areas shows that the gaps between these columnar crystals were filled with a scattered distribution of short rod-shaped crystals. The NaF group had Ca/F of 11.40 ± 1.88 and Ca/P of 1.53 ± 0.06 (Fig. 1J). According to an elemental investigation, the crystals were probably composed of fluorohydroxyapatite (FHA) and CaF_2 [18].

AFM morphology

For the AFM images, the surface of the intact enamel was smooth, with some fine scratches visible. The 3D image showed some areas of roughness (Fig. 2A, B). The roughness was 21.10 ± 8.19 nm. After acid eroding, the enamel surface exhibited a high degree of surface porosity. It showed the classic fish-scale surface morphology of demineralized enamel and the typical prismatic structure of enamel (Fig. 2C, D). This change in morphological aspect was also manifested in the change in surface roughness, which increased significantly from 21.1 nm to 358.6 nm. After pH-cycling remineralization, all three groups had a deposit on the enamel surface. Damage was filled in and repaired, the height difference between the enamel and internal rods was reduced and the roughness was significantly reduced. The AFM 2D image of the DDW group showed a heterogeneous distribution of color on the enamel surface, indicating a highly undulating surface (Fig. 2E). The AFM 3D image showed a phenomenon resembling a fish scale after acid eroding. The enamel surface was deposited with a layer of disordered minerals and was overall uneven and mountainous in appearance. The surface pores had been repaired to some extent, but their depth was still large (Fig. 2F). The surface roughness was significantly lower (114 ± 21.13) compared to after acid eroding. On the basis of the SEM images, the AFM images also provide further evidence of the effect of TRAP on enamel remineralization. The AFM 2D image of the peptide TRAP group showed a more even distribution of color, indicating a flatter surface of the enamel (Fig. 2G). The AFM 3D image showed a typical deposit layer on the enamel surface, with a large number of closely spaced protruding rod-shaped crystal structures. The enamel rods were slightly visible, but the pores were well-filled. The structure of the new crystals was similar to that of natural enamel. Both enamel rods and interstitial enamel rods were repaired (Fig. 2H). The surface roughness increased to (76.8 ± 22.1). The AFM 2D and 3D images of the NaF group showed a flat surface. This demonstrated better repair of enamel rods and interstitial enamel rods (Fig. 2I, J). The surface roughness increased to (73.72 ± 15.98).

A comparison of the roughness values of the surface of intact, eroded, and remineralized enamels showed that the eroded enamel surface roughness increased significantly than the intact ($p < 0.05$) and the remineralized enamel surface roughness reduced significantly than the

Wen *et al. BMC Oral Health*   (2024) 24:1054

Page 5 of 11
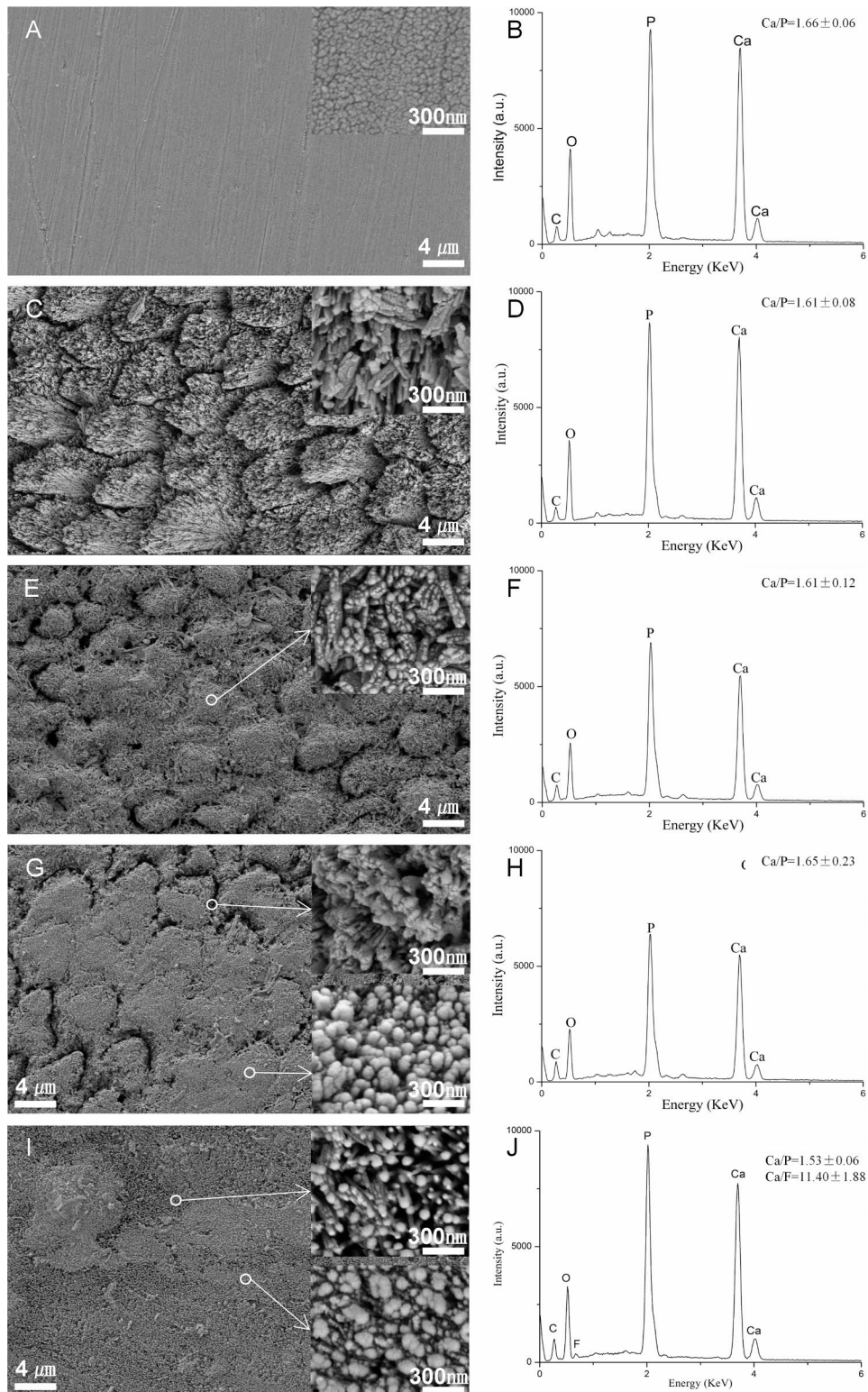
Fig. 1 I SEM images and EDXS analyses of the surface of the enamel. Intact enamel: **(A**, **B)**. eroded enamel: **(C**, **D)**. DDW group: **(E**, **F)**. TRAP group: **(G**, **H)**. NaF group: **(I**, **J)**

Wen *et al. BMC Oral Health*   (2024) 24:1054

Page 6 of 11
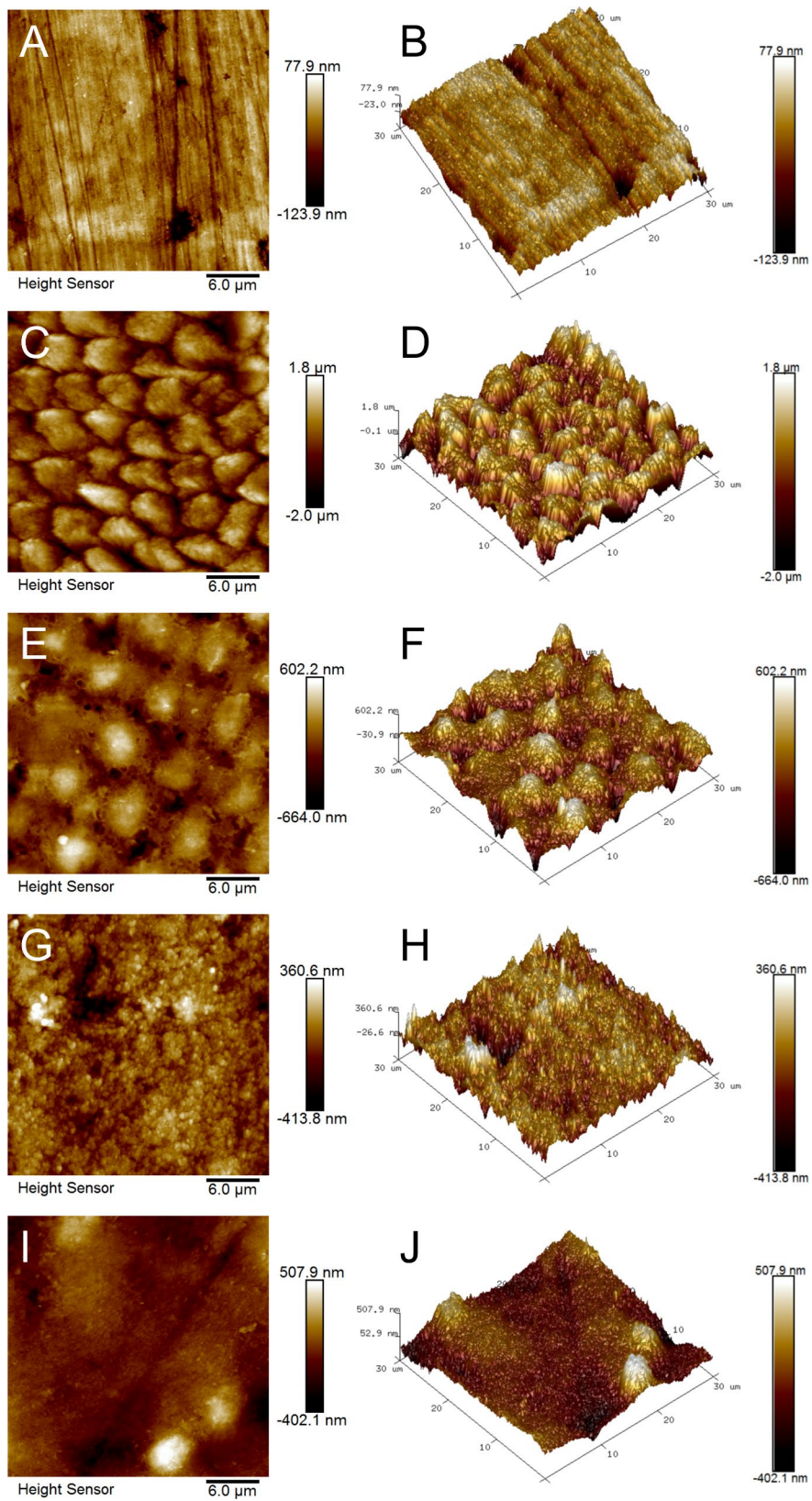
Fig. 2 l AFM images of the surface of the tooth enamel. Intact enamel: **(A**, **B)**. eroded enamel: **(C**, **D)**. DDW group: **(E**, **F)**. TRAP group: **(G**, **H**. NaF group: **(I**, **J)**

remineralized ($p<0.05$). The differences between the two groups were statistically significant ($p<0.05$), except for the TRAP and NaF groups ($p>0.05$) (Fig. 3).

FT-IR Spectra and XRD Spectra

The FT-IR (Fig. 4) and XRD (Fig. 5) spectra show that the nascent mineral phases of the DDW and TRAP groups are mainly HA. The nascent mineral phases of the NaF group are mainly FAP. After pH-cycling, the FT-IR (Fig. 4) spectrum shows a clear PO_4^{3-} band (597.97 cm^{-1} and 986.59 cm^{-1}) indicating the formation of HA. In addition, the results of the peptide TRAP group showed that amide I (1650 cm^{-1}) was detected. The results of the NaF group showed that a new wave peak (742 cm^{-1})was detected. This is due to the F^{-} substituted OH. The XRD spectra of the nascent crystals after remineralization are shown in Fig. 5, indicating the presence of apatite crystals. The diffraction peaks at $2\Theta = 25.8°$, 32.2° and 34.1° corresponding to the reflections of HA (002), (112), and (202) are observed in the HA diffraction bands for all sets of results. Since the XRD spectra did not reveal CaF_2 diffraction bands, combined with the results of the EDXS, we infer that the crystals of the NaF group are FHA.

Discussion

The pH-cycling model was used for the first time in this study to investigate the changes in surface morphology after the remineralization of eroded enamel by the peptide TRAP. The results showed that there were significant differences in the surface characteristics of the three groups of test samples and that the peptide TRAP had a lower remineralizing effect on eroded enamel than sodium fluoride and a higher impact than DDW. The peptide TRAP can promote the remineralization of enamel.

We used the pH-cycling model reported by White DJ et al. to investigate the remineralization effect of TRAP on eroded enamel surfaces in this study. The model consists of a demineralizing solution and a simple remineralizing solution soaked in enamel samples, and the specimens were subjected to cyclic demineralization and remineralization using an artificial mouth to simulate the physiological state of the mouth. Remineralization to repair surface damage to demineralized enamel in the presence of fluoride or TRAP, using appropriately modulating Ca^{2+}/PO_4^{3-} ion concentrations [16]. As a large amount of saliva is required to perform this study in an artificial mouth, a remineralizing solution was primarily chosen to replace human saliva. Mayumi Iijima used a cation-selective membrane model to compare the types of surface crystals formed after remineralization of demineralized
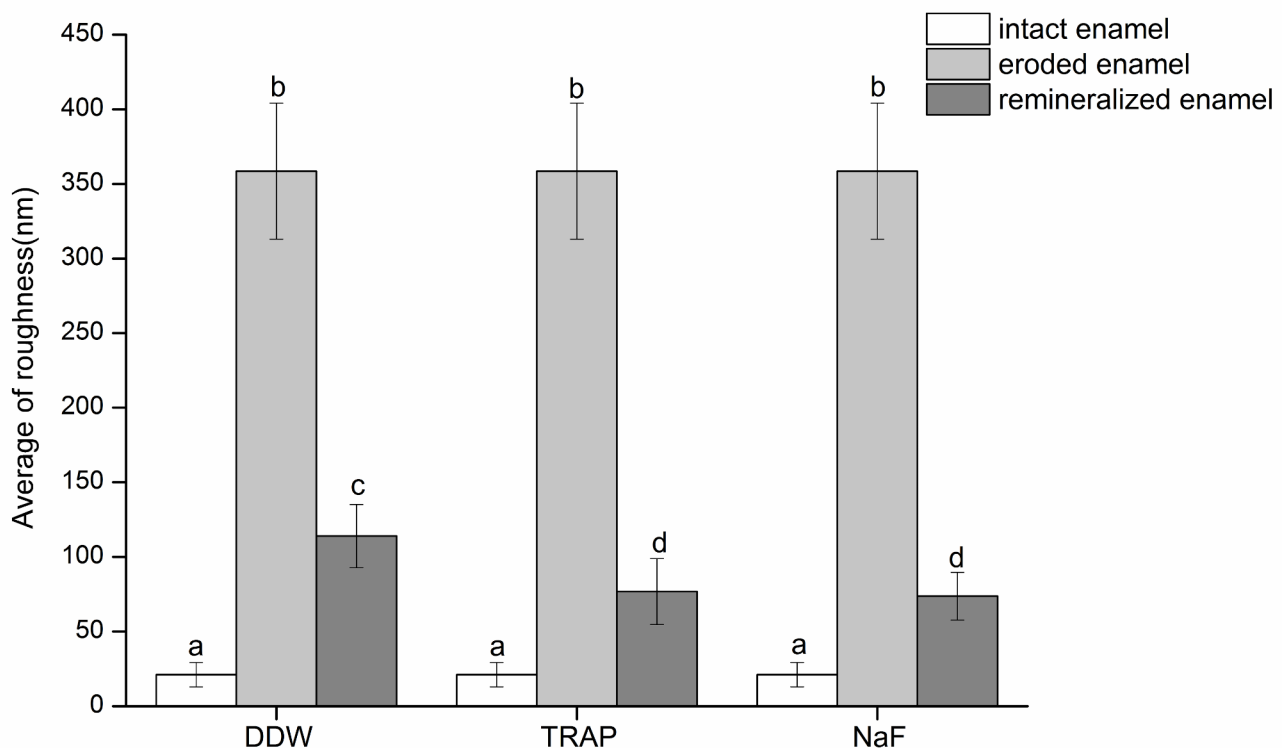
Fig. 3 | SD bars labeled with different letters show a statistically significant difference, *P* < 0.05
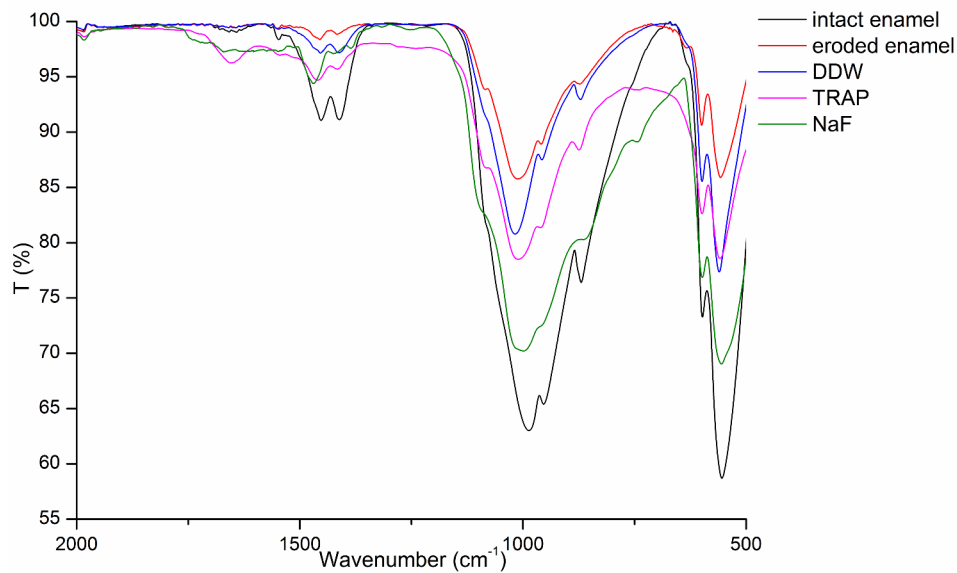
Fig. 4 I FT-IR images of the surface of the buccal surface of deionized water-treated demineralized enamel, TRAP-treated demineralized enamel, and sodium fluoride-treated demineralized enamel after 14 days of pH-cycling, intact enamel and eroded enamel
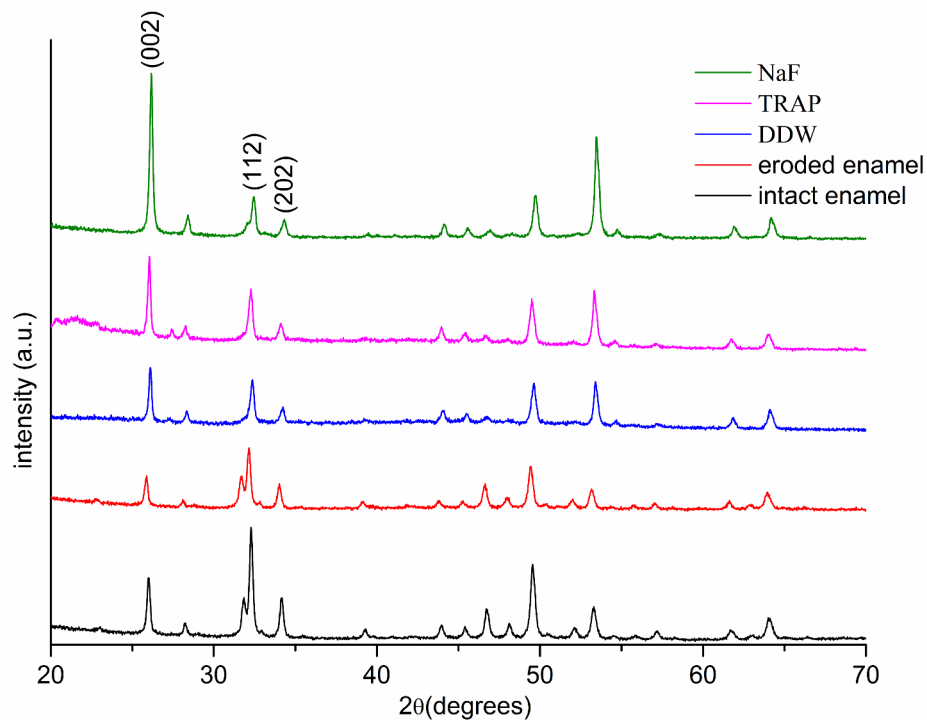
Fig. 5 I XRD images of the buccal surface of deionized water-treated demineralized enamel, TRAP-treated demineralized enamel, and sodium fluoride-treated demineralized enamel after 14 days of pH-cycling, intact enamel and eroded enamel

enamel at different F^- concentrations. At low concentrations of F^- (<2 ppm), the newly formed crystals were mostly OCP or a mixture of OCP and HA. At a concentrations of 2 ppm, FHA can be formed. The FT-IR and XRD results are also consistent with their results in this study [6].

The effect of TRAP on the surface of enamel after being eroded was compared with that of DDW and NaF by SEM. TRAP and NaF clearly showed the potential for remineralization, with changes at the level of surface morphology, maintaining a rough and homogeneous appearance. The enamel crystals were discontinuous

Wen *et al. BMC Oral Health*   (2024) 24:1054

Page 9 of 11

and broken at the surface after being eroded, which is consistent with the typical pattern of type 2 demineralization and was confirmed by the Ca/P ratio results [19, 20]. After the pH-cycling, apatite coatings were formed on the eroded enamel surfaces. The enamel surface of the DDW group was seen to be porous with a haphazard, scattered distribution of loose banded crystalline coatings, in agreement with the results of Sami Dogan et al. [21]. The enamel surface may deposit calcium and phosphorus ions derived from supersaturated solutions. Still, they are too weakly bound to the enamel substrate and are easily dislodged during pH-cycling remineralization. The enamel surface of the polypeptide TRAP group shows a structure similar to that of natural enamel. The border between the restored enamel and the eroded enamel reflects the successful growth of a new HA layer, with the new needle-like crystals arranged in parallel and tightly packed, growing in a manner consistent with the orientation of the existing enamel crystals. This organized crystal bundle was also observed in the previously reported remineralization pattern of the recombinant amelogenin polypeptide [22]. Previous research has demonstrated that one of the most crucial properties the material should possess for enamel remineralization is a significant affinity with the substratum [23]. In a previous study, we found that TRAP has a good affinity for calcium ions and binds to them [14]. In our study, the FT-IR test results for the treated demineralized enamel samples in our investigation showed typical peaks of the TRAP peptide, showing that TRAP had been adsorbed on the enamel surface. As a result, we propose that TRAP may help remineralize enamel by interacting with Ca^{2+} to produce a TRAP-ACP complex that strongly binds the developing ACP to the enamel and subsequently transforms it into HA. The enamel surface of the NaF group was flat and formed a large number of relatively regular columnar crystals. This is mainly due to the fact that the addition of F^- increases the crystalline properties of HAP and the structure of the HA molecule becomes more dense. This is similar to the results of Longjiang Ding et al. [15].

According to the AFM images (Fig. 3), after the pH-cycling, remineralization caused the deposition of crystalline material and a decrease in surface roughness, which greatly decreased the depth of the erosion cavities. PH-cycling resulted in a distinct surface layer on the surface of the TRAP and NaF groups enamel, whereas no surface layer was evident on the surface of the enamel treated with DDW only. The AFM images of the DDW group showed minimal morphological changes on the enamel surface compared to the eroded enamel surface, which still showed a porous fish scale structure. This is similar to the results of Lippert et al. [24]. Lesions in the TRAP and NaF groups were significantly shallower than in the DDW group. These results provide direct evidence that TRAP and NaF promote remineralization. The enamel surface roughness was similar for the TRAP group and NaF group after pH-cycling. However, combined with SEM and AFM topographic analysis, the enamel surface was flatter and had more tissue recovery in the NaF group. On the enamel surface of the polypeptide TRAP group, the crystals showed typical nano-HA microcrystals with a needle-like morphology, arranged in parallel and densely packed along the c-axis, forming the prototype of enamel prismatic bundles. The enamel prismatic crystals are regularly aligned in the same direction and grow in a manner consistent with the existing orientation of enamel crystals, successfully mimicking the texture of natural enamel. This may be related to the fact that TRAP contains the exogenous lectin-binding motif "PYTSYGYEPMGGW", "A-domain" of amelogenin self-assembly, and the unique phosphate group of amelogenin. Combined lectin properties may have a function to determine the direction of the "nanosphere", which will affect the orientation of the microcrystals [25]. TRAP contains all the "A-domain" of the amelogenin self-assembly. Additionally, in vitro and in vivo studies have shown that the "A-domain" is removed, which interferes with amelogenin self-assembly [26, 27]. This suggests that TRAP can self-assemble to form 'nanospheres'. When HA crystals adsorbed on particular surfaces, the acidic amino acids may have controlled how the crystals were oriented [28]. The phosphate group plays an important role in stabilizing ACP, inhibiting its premature precipitation, and regulating the formation of ordered hydroxyapatite crystals, as verified in results obtained by comparing naturally phosphorylated full-length (P173) and dephosphorylated P173 and LRAP (+P, -CT) and LRAP (-P, -CT) [29, 30].

Combined with the results of elemental analysis, the FT-IR (Fig. 4) and XRD (Fig. 5) Spectra indicate that the mineral phases of the DDW and TRAP groups are predominantly HA. The NaF group is predominantly FAP. The remineralized coating of the TRAP group contains protein and phosphate, as shown by FT-IR analysis. The peptide TRAP could adsorb on the enamel surface. By combining the findings from the AFM, SEM, and FTIR experiments, we now propose that TRAP can depend on the interaction of phosphate groups with Ca^{2+} to form TRAP-ACP complexes and temporarily stabilize ACP, which can then encourage the deposition of phosphorus and calcium on the enamel surface and also enter the interior of the lesion through the pores of demineralized enamel lesions, eventually resulting in their transformation into hydroxyapatite crystals. As a result of the F^- substituted OH, the original hydroxyl vibrational mode changes, and splits, so that a new peak appears at 742 cm^{-1} in the NaF group.

The XRD results show that the diffraction peak positions are essentially the same for all three sets of samples,

Wen *et al. BMC Oral Health*   (2024) 24:1054

Page 10 of 11

indicating that the addition of TRAP and fluorine did not affect the mineral phase and that the crystals of HA remained essentially unchanged in their dense hexagonal structure. The increase in the spreading peak at $2\Theta = 20–22°$ may indicate the presence of amorphous calcium phosphate in the TRAP group [31]. This spreading may also be the result of the presence of smaller apatite crystals. The XRD results for NaF partially shift the reflection peak to the right, a reflection pattern similar to that previously reported for fluorohydroxyapatite [32]. Because when a HA layer is developed on a layered OCP precursor in the presence of F ions, as in the structure described by Iijima et al., this shift may represent an overlap of fluorinated HA and OCP [6].

These results indicate that the TRAP peptide remineralized the eroded enamel more efficiently than DDW but less efficiently than NaF. However, in the TRAP peptide group, after the remineralization of eroded enamel, the crystals deposited on the surface of the enamel have the same morphology and growth direction as normal enamel.

Conclusions

This study demonstrates that the peptide TRAP can promote the remineralization of eroded enamel surfaces. TRAP binds to the enamel surface, temporarily stabilizes ACP, controls further crystallization of HA on the original enamel crystals, promotes the remineralization of eroded enamel, and restores the original enamel surface. It is suggested that it has significant potential for remineralization, and provides a promising biomaterial for the remineralization treatment of enamel lesions.

Author contributions
MW and JC took part in the design of this study, and they both conducted the data analysis. MW and QB carried out the experiment and collected important background information. Yi L and Ya L provided assistance for data collection and analysis. DM and Ya L carried out a literature search, data collection, and manuscript editing. All authors reviewed the manuscript.

Data availability
Upon reasonable request, the corresponding author will provide the datasets used and/or analyzed in the current work.

Declarations

Ethics approval and consent to participate
This study protocol was reviewed and approved by the Ethics Committee of the First Affiliated Hospital of Zhengzhou University, approval number [2021-ky-1050-002]. According to the decision of the Ethics Committee of the First Affiliated Hospital of Zhengzhou University, the study has been granted an exemption from requiring written informed consent.

Consent for publication
Not applicable.

Competing interests
The authors declare no competing interests.

References

1. Dawes C. What is the critical pH and why does a tooth dissolve in acid? J Can Dent Assoc. 2003;69(11):722–4.
2. Lussi A, Jaggi T, Scharer S. The influence of different factors on in vitro enamel erosion. Caries Res. 1993;27(5):387–93.
3. Huang Z, Newcomb CJ, Bringas P Jr., Stupp SI, Snead ML. Biological synthesis of tooth enamel instructed by an artificial matrix. Biomaterials. 2010;31(35):9202–11.
4. Dai LL, Mei ML, Chu CH, Lo ECM. Mechanisms of Bioactive Glass on Caries Management: a review. Mater (Basel) 2019, 12(24).
5. Cicciu M, Fiorillo L, Cervino G. Chitosan Use in Dentistry: a systematic review of recent clinical studies. Mar Drugs 2019, 17(7).
6. Iijima M, Tohda H, Suzuki H, Yanagisawa T, Moriwaki Y. Effects of F- on apatite-octacalcium phosphate intergrowth and crystal morphology in a model system of tooth enamel formation. Calcif Tissue Int. 1992;50(4):357–61.
7. Philip N. State of the art Enamel Remineralization systems: the Next Frontier in Caries Management. Caries Res. 2019;53(3):284–95.
8. Wang H, Xiao Z, Yang J, Lu D, Kishen A, Li Y, Chen Z, Que K, Zhang Q, Deng X, et al. Oriented and ordered biomimetic remineralization of the Surface of Demineralized Dental Enamel using HAP@ACP nanoparticles guided by Glycine. Sci Rep. 2017;7:40701.
9. Bartlett JD, Simmer JP. Proteinases in developing dental enamel. Crit Rev Oral Biol Med. 1999;10(4):425–41.
10. Dissanayake SSM, Ekambaram M, Li KC, Harris PWR, Brimble MA. Identification of key functional motifs of native amelogenin protein for Dental Enamel Remineralisation. Molecules 2020, 25(18).
11. Paine ML, Snead ML. Protein interactions during assembly of the enamel organic extracellular matrix. J Bone Min Res. 1997;12(2):221–7.
12. Chu J, Feng X, Guo H, Zhang T, Zhao H, Zhang Q. Remineralization efficacy of an amelogenin-based synthetic peptide on Carious Lesions. Front Physiol. 2018;9:842.
13. Ravindranath RM, Tam WY, Nguyen P, Fincham AG. The enamel protein amelogenin binds to the N-acetyl-D-glucosamine-mimicking peptide motif of cytokeratins. J Biol Chem. 2000;275(50):39654–61.
14. Li Y, Li Y, Bai Q, Wen M, Ma D, Lin Y, Chu J. Recombinant amelogenin peptide TRAP promoting remineralization of early enamel caries: an in vitro study. Front Physiol. 2023;14:1076265.
15. Ding L, Han S, Wang K, Zheng S, Zheng W, Peng X, Niu Y, Li W, Zhang L. Remineralization of enamel caries by an amelogenin-derived peptide and fluoride in vitro. Regen Biomater. 2020;7(3):283–92.
16. White DJ. Reactivity of fluoride dentifrices with artificial caries. I. effects on early lesions: F uptake, surface hardening and remineralization. Caries Res. 1987;21(2):126–40.
17. ten Cate JM, Duijsters PP. Influence of fluoride in solution on tooth demineralization. II. Microradiographic data. Caries Res. 1983;17(6):513–9.
18. Mei ML, Nudelman F, Marzec B, Walker JM, Lo ECM, Walls AW, Chu CH. Formation of Fluorohydroxyapatite with Silver Diamine Fluoride. J Dent Res. 2017;96(10):1122–8.
19. Hicks MJ, Silverstone LM. Internal morphology of surface zones from acid-etched caries-like lesions: a scanning electron microscopic study. J Dent Res. 1985;64(11):1296–301.
20. Kwak SY, Litman A, Margolis HC, Yamakoshi Y, Simmer JP. Biomimetic enamel regeneration mediated by Leucine-Rich Amelogenin Peptide. J Dent Res. 2017;96(5):524–30.
21. Dogan S, Fong H, Yucesoy DT, Cousin T, Gresswell C, Dag S, Huang G, Sarikaya M. Biomimetic tooth repair: amelogenin-derived peptide enables in Vitro Remineralization of Human Enamel. ACS Biomater Sci Eng. 2018;4(5):1788–96.
22. Moradian-Oldak J, Iijima M, Bouropoulos N, Wen HB. Assembly of amelogenin proteolytic products and control of octacalcium phosphate crystal morphology. Connect Tissue Res. 2003;44(Suppl 1):58–64.

23. Liu Y, Ding C, He L, Yang X, Gou Y, Xu X, Liu Y, Zhao C, Li J, Li J. Bioinspired heptapeptides as functionalized mineralization inducers with enhanced hydroxyapatite affinity. J Mater Chem B. 2018;6(13):1984–94.

24. Lippert F, Parker DM, Jandt KD. In vitro demineralization/remineralization cycles at human tooth enamel surfaces investigated by AFM and nanoindentation. J Colloid Interface Sci. 2004;280(2):442–8.

25. Paine ML, Snead ML. Tooth developmental biology: disruptions to enamel-matrix assembly and its impact on biomineralization. Orthod Craniofac Res. 2005;8(4):239–51.

26. Lench NJ, Winter GB. Characterisation of molecular defects in X-linked amelogenesis imperfecta (AIH1). Hum Mutat. 1995;5(3):251–9.

27. Collier PM, Sauk JJ, Rosenbloom SJ, Yuan ZA, Gibson CW. An amelogenin gene defect associated with human X-linked amelogenesis imperfecta. Arch Oral Biol. 1997;42(3):235–42.

28. Matsumoto T, Okazaki M, Inoue M, Sasaki J, Hamada Y, Takahashi J. Role of acidic amino acid for regulating hydroxyapatite crystal growth. Dent Mater J. 2006;25(2):360–4.

29. Wiedemann-Bidlack FB, Kwak SY, Beniash E, Yamakoshi Y, Simmer JP, Margolis HC. Effects of phosphorylation on the self-assembly of native full-length porcine amelogenin and its regulation of calcium phosphate formation in vitro. J Struct Biol. 2011;173(2):250–60.

30. Le Norcy E, Kwak SY, Wiedemann-Bidlack FB, Beniash E, Yamakoshi Y, Simmer JP, Margolis HC. Leucine-rich amelogenin peptides regulate mineralization in vitro. J Dent Res. 2011;90(9):1091–7.

31. Fan Y, Sun Z, Moradian-Oldak J. Controlled remineralization of enamel in the presence of amelogenin and fluoride. Biomaterials. 2009;30(4):478–83.

32. Chen Y, Miao X. Thermal and chemical stability of fluorohydroxyapatite ceramics with different fluorine contents. Biomaterials. 2005;26(11):1205–10.

Publisher's note